



## Structural investigation of $\text{Pb}(\text{Mo}_x\text{W}_{1-x})\text{O}_4$ solid solutions via X-ray and neutron diffraction



G.M. Kuz'micheva<sup>a</sup>, I.A. Kaurova<sup>a,\*</sup>, A.A. Brykovskiy<sup>a</sup>, V.B. Rybakov<sup>b</sup>, Yu. N. Gorobets<sup>c</sup>, A.N. Shekhovtsov<sup>c</sup>, A. Cousson<sup>d</sup>

<sup>a</sup> Department of Materials Science and Technology of Functional Materials and Structures, Moscow Technological University, MITHT, Vernadskogo pr. 86, Moscow 119571, Russia

<sup>b</sup> Department of Chemistry, Lomonosov State University, Vorobyovy Gory, Moscow 119992, Russia

<sup>c</sup> Department of Ferroelectric and Laser Single Crystals, Institute for Single Crystals of NAS of Ukraine, Lenin 60, Ave., Kharkov 61001, Ukraine

<sup>d</sup> Laboratoire Leon Brillouin, Cea/Saclay, Gif-sur-Yvette, Cedex 91191, France

### ARTICLE INFO

#### Article history:

Received 5 October 2015

Received in revised form 19 February 2016

Accepted 22 February 2016

Available online 24 February 2016

#### Keywords:

Optical materials

Crystal growth

X-ray diffraction

Neutron diffraction

Crystal structure

### ABSTRACT

$\text{PbMo}_x\text{W}_{1-x}\text{O}_4$  single-crystal solid solutions with  $x=0.2, 0.5, 0.8$  have been grown by the Czochralski method in air atmosphere from the initial charge with over-stoichiometric amount of  $\text{YNbO}_4$  (15 wt%). X-ray and neutron single-crystal and X-ray powder (Rietveld method) diffraction investigations of  $\text{PbMo}_x\text{W}_{1-x}\text{O}_4$  crystals indicate bulk inhomogeneity of their compositions, absence of color centers, and deviation of refined compositions from initial ones: the  $\text{Nb}^{5+}$  and  $\text{Y}^{3+}$  contents as well as oxygen vacancies content increase with increasing  $x$  in  $\text{PbMo}_x\text{W}_{1-x}\text{O}_4$ . It was found that  $\text{PbMo}_x\text{W}_{1-x}\text{O}_4$  with  $x=0.2, 0.5, 0.8, 1.0$  crystallizes in the scheelite-type structure with space group  $I4_1/a$ , unlike crystal with  $x=0$ , which is characterized by the symmetry reduction to space group  $I\bar{4}$  caused by ordering of oxygen vacancies. The correlation between the  $a$  and  $c$  unit cell parameters and composition of cation sites, dodecahedral and tetrahedral, and deficiency of oxygen site was revealed.

© 2016 Elsevier Ltd. All rights reserved.

## 1. Introduction

Lead molybdates and tungstates,  $\text{PbMoO}_4$  (PMO) and  $\text{PbWO}_4$  (PWO), respectively, with the general chemical formula  $\text{PbTO}_4$  ( $T=\text{Mo}, \text{W}$ ) (PTO) are related to optical materials belonging to the crystal family with  $\text{CaWO}_4$  scheelite-type structure (space group  $I4_1/a, Z=4$ ) [1], where the Ca (Pb) atoms are located in  $\text{CaO}_8$  ( $\text{PbO}_8$ ) dodecahedra (square antiprism with refracted upper faces; the symmetry of dodecahedron is  $S_4$ ) with coordination number (CN) - 4 + 4, i.e., with two sets of different cation-anion interatomic distances ( $d_{A1-O} > d_{A2-O}$ , Å) (Fig. 1a) and the W (Mo) atoms are located in  $\text{WO}_4$  ( $\text{MoO}_4$ ) tetrahedra (CN=4; the symmetry of tetrahedron is  $S_4$ ) with an equal cation-anion interatomic distances but with two different O—O ones ( $d_1 < d_2$ , Å) (Fig. 1b). Each O atom is coordinated by two Ca (Pb) atoms and one W (Mo) atom (CN=3).

PMO crystals are currently used in acousto-optical devices, such as modulators, deflectors and phase shifters [2], whereas PTO crystals are used as scintillation detectors [3,4]. In addition, PTO crystals demonstrate high Raman cross section that provides

effective energy conversion into Stokes and anti-Stokes components. It allows using these crystals in Raman lasers, where active laser medium also acts as a converter of laser radiation [5]. Simultaneous laser operation and stimulated Raman scattering (SRS) were found for  $\text{PbMoO}_4:\text{Nd}^{3+}$  and  $\text{PbWO}_4:\text{Nd}^{3+}$  crystals under different types and conditions of pumping [6,7].

Unlike  $\text{PbMoO}_4$  and  $\text{PbWO}_4$  crystals, for which spectral lines of the first and second Stokes components were observed,  $\text{PbMo}_x\text{W}_{1-x}\text{O}_4$  (PMWO) ( $x=0.5$ ) single crystal shows a set of lines in the spectrum due to the conversion of radiation into the first and second Stokes components on the molybdate and tungstate anionic complexes, and their combination [8].

The use of PTO and PMWO crystals in the above mentioned areas may be limited by an additional optical absorption caused by the presence of point defects and their associates in the crystal structures: antisite defects  $\text{Pb}_{\text{Mo}}^{n*}$  (the presence of  $\text{Pb}^{2+}$  ions in the  $\text{Mo}^{6+}$  sites), charge exchange of the cations  $\text{Pb}^{2+} + \text{Mo}^{6+} \rightleftharpoons \text{Pb}^{3+} + \text{Mo}^{5+}$  [9], color centers  $(V_{\text{Mo}}^{n+}, \text{nh}^*)^x$  or  $(V_{\text{Pb}}^{n+}, \text{nh}^*)^x$  (vacancies in the  $\text{Mo}^{6+}$  or  $\text{Pb}^{2+}$  sites, respectively, and localized holes) [10,11],  $(V_{\text{O}}^{n*}, \text{ne}')^x$  (vacancies in the  $\text{O}^{2-}$  sites and localized electrons) [11], and partial transition  $\text{Mo}^{6+} \rightarrow \text{Mo}^{5+}$  [12].  $\text{YNbO}_4$  is added into the initial charge to prevent the appearance of color and formation of point defects in PMWO crystals [13].

\* Corresponding author.

E-mail address: [kaurchik@yandex.ru](mailto:kaurchik@yandex.ru) (I.A. Kaurova).

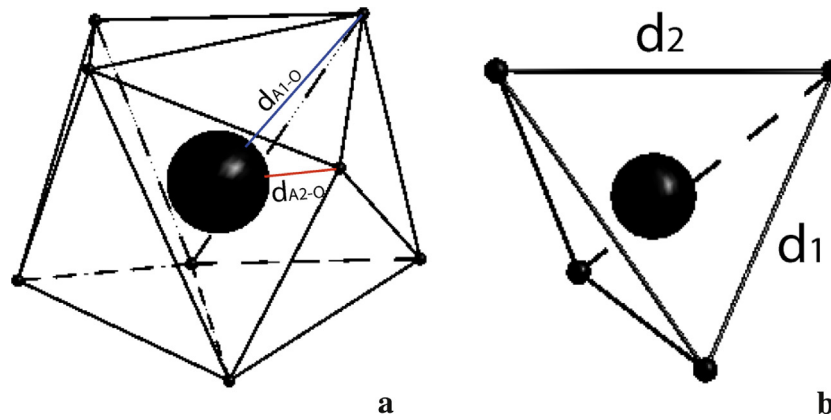


Fig. 1. Coordination polyhedra in  $\text{CaWO}_4$ -type structure:  $\text{CaO}_8$  (a) and  $\text{WO}_4$  (b).

The purpose of our study was to determine  $\text{YNbO}_4$  influence on structural parameters of  $\text{PbMo}_x\text{W}_{1-x}\text{O}_4$  single crystals.

## 2. Experimental technique

$\text{PbMoO}_4$  and  $\text{PbWO}_4$  single crystals [12] as well as  $\text{PbMo}_x\text{W}_{1-x}\text{O}_4$  solid solutions with  $x=0.2$  (PMWO-1),  $x=0.5$  (PMWO-2),  $x=0.8$  (PMWO-3) were grown by the Czochralski method on the “Analogue” growth equipment with a weight sensor in the Pt crucible in an air (PMO-A, PWO-A, PMWO) and nitrogen (PM O- $\text{N}_2$ , PW O- $\text{N}_2$ ) atmospheres (Tables 1, 2). Extra pure grade  $\text{PbO}$ ,  $\text{WO}_3$ ,  $\text{Nb}_2\text{O}_5$  and  $\text{Y}_2\text{O}_3$  and GR grade  $\text{MoO}_3$  oxides were taken in a stoichiometric ratio for initial charge preparation. For PMWO growth, over-stoichiometric amount of  $\text{YNbO}_4$  was added into the initial charge. Ceramic technology was used to grow crystals. Growth conditions were identical to those described in [13]:  $\langle 001 \rangle$  growth direction; temperature gradient  $T_z = 50\text{--}70$  deg/cm; rotation rate  $\omega = 20\text{--}30$  rpm; pulling rate  $V_z = 1\text{--}3$  mm/h; crystallization front was flat or slightly convex. Single crystals with a diameter of 15–20 mm and a length of 60 mm were free of impurity phases, macro-inclusions, cracks, and bubbles.

The X-ray powder diffraction data for samples ground to a powder ( $\sim 100$  mg) were collected in reflection mode at room temperature on HZG-4 (flat graphite monochromator) X-ray powder diffractometer using  $\text{CuK}\alpha$  radiation and a diffracted beam (step-scan mode; the count time was 15 s and the step size was  $0.02^\circ$ ) in the  $2\theta$  angle range of  $15^\circ\text{--}140^\circ$ . To prevent any orientation predominating, the samples were rotated during X-ray data collection. The preliminary X-ray powder diffraction data processing was performed using the FullProf-2007 software package [14]. The qualitative phase analysis of the samples, which was performed with the use of the PCPDFWIN automatic search software for reading the PDF-2 database, showed that all samples were single phase. All calculations intended for refinement of the composition and structure of powdered samples were performed by the Rietveld method (RM) with the DBWS-9411 program [15].

Table 1

Time and temperature modes of synthesis of PMO, PWO phases and PMWO solid solutions.

Sample	Temperature, $^\circ\text{C}$	Time, h	Phase content, wt%
$\text{PbWO}_4$ (PWO)	700	10	98
$\text{PbMoO}_4$ (PMO)	650		97
$\text{PbMo}_{0.2}\text{W}_{0.8}\text{O}_4$ (PMWO-1)	700		97
$\text{PbMo}_{0.5}\text{W}_{0.5}\text{O}_4$ (PMWO-2)	700		96
$\text{PbMo}_{0.8}\text{W}_{0.2}\text{O}_4$ (PMWO-3)	700		97
$\text{YNbO}_4$	1100		96

The X-ray Diffraction Analysis (XDA) of samples  $\sim 0.1 \times 0.1 \times 0.1$  mm<sup>3</sup> in size was carried out on a STOE Stadi Vari PILATUS 100 K single-crystal diffractometer at room temperature ( $\text{MoK}\alpha$ ). The preliminary X-ray diffraction data processing was carried out using the WinGX pack [16] with a correction for absorption (MULTISCAN).

Neutron Diffraction Analysis (NDA) of samples  $\sim 5 \times 5 \times 5$  mm<sup>3</sup> in size was carried out at room temperature on the four-circle single-crystal diffractometer installed at the hot source (5C2) of the Orphee reactor (LLB, France,  $\lambda = 0.83$  Å).

The crystal structures of all samples were refined by the full-matrix least-squares method in the isotropic and anisotropic approximations for all atoms using the SHELXL-97 software package [17], taking into account the atomic scattering curves for neutral atoms. The technique, described in detail in [18,19], was used for the refinement of crystal structures of samples under investigation due to the correlation between site occupancies and thermal parameters.

## 3. Results and discussion

The unit cell parameter can be used as a structural parameter to qualitatively judge the composition of the crystals. The unit cell parameters were determined for PTO samples of various sizes by different diffraction methods: for powdered crystals ( $\sim 100$  mg)—by the RM; for microparts of the same crystals ( $\sim 0.1 \times 0.1 \times 0.1$  mm<sup>3</sup>)—by single-crystal XDA; for macroparts of the same crystals ( $\sim 5 \times 5 \times 5$  mm<sup>3</sup>)—by single-crystal NDA (Table 2). Table 2 shows that the  $a$  unit cell parameter decreases and the  $c$  unit cell parameter increases from PWO to PMO, regardless of the growth atmosphere, that correlates with the ionic radii of  $\text{W}^{6+}$  ( $r_{\text{W}^{6+}} = 0.44$  Å) and  $\text{Mo}^{6+}$  ( $r_{\text{Mo}^{6+}} = 0.41$  Å) [20]. Such antipath change in the  $a$  and  $c$  unit cell parameters is due to a decrease and increase in the O—O interatomic distances  $d_1$  and  $d_2$  in the  $\text{MoO}_4$  tetrahedron, respectively, with decreasing atomic size in it (Fig. 1b, Table 2).

According to the XDA, NDA and RM [12], the refined compositions of PMO and PWO crystals can be written in the general form as  $(\text{Pb}, \square)\text{MoO}_4$  and  $\text{PbW}(\text{O}, \square)_4$ , i.e., with vacancies ( $\square$ ) in the Pb and O sites, respectively. Comparison of the unit cell parameters of the same samples, obtained in different growth atmospheres (in air—A; in nitrogen— $\text{N}_2$ ) (Table 2), shows that PMO and PWO crystals grown in  $\text{N}_2$  atmosphere are characterized by higher content of vacancies in Pb and O sites, respectively, if compared with those grown in air atmosphere [12] (the  $a$  and  $c$  unit cell parameters decrease symbolically) (Fig. 2). Hence, it is possible that the “radius” of anion vacancies (and, possibly, the “radius” of cation vacancies) is less than the radius of atoms, which

**Table 2**  
Characteristics of the  $\text{PbMoO}_4$  (PMO),  $\text{PbWO}_4$  (PWO),  $\text{PbMo}_x\text{W}_{1-x}\text{O}_4$  (PMWO) samples.

Designation	Charge composition, growth and annealing atmospheres	Color	Unit cell parameters $a, c, \text{\AA}$		
			RM	XDA	NDA
PWO-A	$\text{PbWO}_4$ growth in air, annealing in vacuum	Light yellow Transparent	5.4753(1) 12.0598(8)	5.4612(4) 12.0199(12)	5.4637(1) 12.0490(3)
PW O-N <sub>2</sub>	$\text{PbWO}_4$ growth in N <sub>2</sub> , annealing in vacuum	Light yellow Transparent	5.46011(9) 12.0421(3)	5.4579(5) 12.0540(14)	5.4609(2) 12.0410(4)
PMO-A	$\text{PbMoO}_4$ growth in air, annealing in vacuum	Light yellow	5.4393(3) 12.1126(6)	5.4285(2) 12.0921(7)	5.4337(4) 12.1017(6)
PM O-N <sub>2</sub>	$\text{PbMoO}_4$ growth in N <sub>2</sub> , annealing in vacuum	Light yellow	5.4382(4) 12.1107(9)	5.4282(5) 12.0595(14)	5.4311(1) 12.0946(2)
PMWO-1	$\text{PbMo}_{0.2}\text{W}_{0.8}\text{O}_4^a$ growth in air, annealing in vacuum	Colorless Transparent	5.4510(2) 12.0801(4)	5.4411(4) 12.0261(12)	5.4468(2) 12.0679(4)
PMWO-2	$\text{PbMo}_{0.5}\text{W}_{0.5}\text{O}_4^a$ growth in air, annealing in vacuum	Colorless Transparent	5.4483(3) 12.0863(9)	5.4350(5) 12.0926(15)	5.4406(3) 12.0700(3)
PMWO-3	$\text{PbMo}_{0.8}\text{W}_{0.2}\text{O}_4^a$ growth in air, annealing in vacuum	Colorless Transparent	5.4447(4) 12.0789(5)	5.4398(3) 12.0534(9)	5.4296(3) 12.0629(4)

<sup>a</sup> Over-stoichiometric  $\text{YNbO}_4$  (15 wt%) was added into the initial charge.

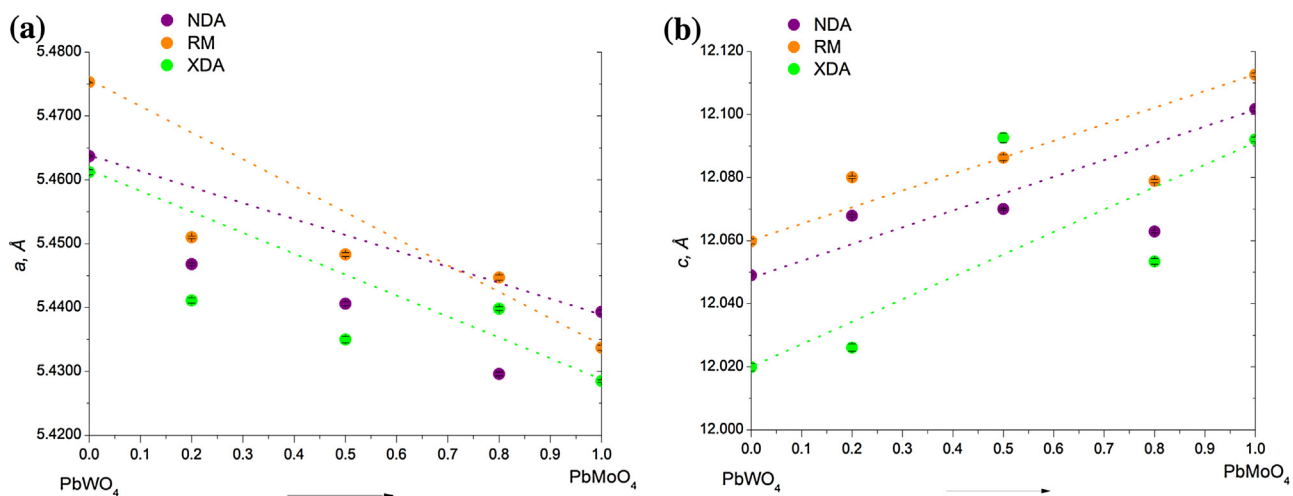


**Fig. 2.** The relationship between the  $a$  (a) and  $c$  (b) unit cell parameters and the initial composition of the  $\text{PbMo}_x\text{W}_{1-x}\text{O}_4$  solid solutions.

is consistent with [21]: “radius” of oxygen vacancy in gadolinium–gallium garnet is 95% of the oxygen atomic radius.

Thus, it is possible to distinguish two main reasons that may influence the behavior of the  $a$  and  $c$  unit cell parameters of  $\text{PbMo}_x\text{W}_{1-x}\text{O}_4$  solid solutions: change in the tetrahedron size under isomorphous substitution of atoms in this site (an antitabite type of dependence), and the presence of vacancies in the dodecahedral (and, possibly, isomorphous substitution of atoms in the same site) and oxygen sites (a symmetrical type of dependence). Undoubtedly, one of two factors prevails. Depending on the method of investigation, the correlation between the Mo content in  $\text{PbMo}_x\text{W}_{1-x}\text{O}_4$  solid solution, grown in air atmosphere (PMWO-A), and the  $a$  and  $c$  unit cell parameters may be described in a linear approximation by the following equations:  $a = 5.4393x + 5.4753(1-x)$  (Eq. 1) and  $c = 12.1126x + 12.0598(1-x)$  (Eq. 2) (RM),  $a = 5.4285x + 5.4612(1-x)$  (Eq. 3) and  $c = 12.1126x + 12.0598(1-x)$  (Eq. 4) (XDA),  $a = 5.4337x + 5.4637(1-x)$  (Eq. 5) and  $c = 12.1017x + 12.049(1-x)$  (Eq. 6) (NDA). All changes in the  $x\text{PbMoO}_4-(1-x)\text{PbWO}_4$  system can be analyzed based on these equations.

For  $\text{PbMo}_x\text{W}_{1-x}\text{O}_4$  solid solutions in the range of compositions  $x = 0.2, 0.5, 0.8$ , a qualitative agreement between the character of changes in the unit cell parameters, determined by the RM and NDA on a relatively large amount of samples taken from the same parts of the crystals, is observed. It should be mentioned that the

quantitative variation of the unit cell parameters may be due to the experimental conditions: different angular ranges, the number of diffraction reflections taken for the refinement, etc. [22] (Fig. 2).

It should be noted that the  $a$  unit cell parameters of PMWO-1, PMWO-2, PMWO-3 solid solutions lie on a straight line ( $a = 5.4428x + 5.4532(1-x)$  (Eq. 7) according to the RM) or almost straight line ( $a = 5.4247x + 5.4533(1-x)$  (Eq. 8) according to the NDA) which are below the lines calculated from Eqs. (1) and (5) (except for PMWO-3 according to the RM) (Fig. 2). The  $a$  unit cell parameters decrease with increasing Mo content in the initial composition ( $r_{\text{Mo}} < r_{\text{W}}$ ). The  $c$  unit cell parameter coincides with the theoretical value for the composition  $x = 0.5$  (PMWO-2) and has a positive and negative deviation from a straight lines, calculated by Eqs. (2) and (6), respectively, for compositions with  $x = 0.2$  (PMWO-1) and  $x = 0.8$  (PMWO-3) (Fig. 2). The  $c$  unit cell parameter also decreases from PMWO-1 to PMWO-3. Based on the symmetrical type of dependence of the unit cell parameters of PMWO solid solutions according to the NDA and RM, it can be concluded that the sizes of dodecahedra play a major role in the behavior of the unit cell parameters.

The charge composition can be written in general form as  $(\text{Pb}^{2+}, \text{Y}^{3+})(\text{Mo}^{6+}, \text{W}^{6+}, \text{Nb}^{5+})\text{O}_4$  ( $r_{\text{Y}^{3+}} = 1.02 \text{\AA}$ ,  $r_{\text{Pb}^{2+}} = 1.29 \text{\AA}$ ,  $r_{\text{Nb}^{5+}} = 0.48 \text{\AA}$ ;  $r_{\text{Pb}^{2+}} > r_{\text{Y}^{3+}}$ ,  $r_{\text{Nb}^{5+}} > r_{\text{W}^{6+}} > r_{\text{Mo}^{6+}}$ ) (it should be recalled that 15 wt%  $\text{YNbO}_4$  was added into the initial charge). Based on the correlation between the unit cell parameters and solid solution compositions

**Table 3**  
Crystallographic data, experimental details and parameters of PMWO crystal structure refinement according to the NDA and XDA data.

Chemical formula of the nominal composition	PbMo <sub>x</sub> W <sub>1-x</sub> O <sub>4</sub>					
System, space group, Z	Tetragonal, I4 <sub>1</sub> /a, 4					
Technique	NDA			XDA		
Sample	PMWO-1	PMWO-2	PMWO-3	PMWO-1	PMWO-2	PMWO-3
<i>a</i> , Å	5.4468(2)	5.4406(3)	5.4296(3)	5.4411(3)	5.4350(5)	5.4398(3)
<i>c</i> , Å	12.0679(4)	12.0700(3)	12.0629(4)	12.0261(12)	12.0926(15)	12.0534(9)
<i>V</i> , Å <sup>3</sup>	358.03	357.27(2)	355.62(2)	356.04(2)	357.21(2)	356.68(2)
<i>D<sub>x</sub></i> , g/cm <sup>3</sup>	8.116	7.643	7.186	8.162	7.644	7.607
$\lambda$ , Å	0.828			MoK $\alpha$ ; 0.71073		
Absorption $\mu$ , mm <sup>-1</sup>	0.01			64.97	64.76	64.45
<i>T</i> , K	293					
Sample size, mm	~5 × 5 × 5			~0.2 × 0.2 × 0.2		
Diffractometer	5C2, Orphee reactor			STOE Stadi Vari PILATUS 100 K		
Type of scan	$\omega$					
$\theta_{\max}$ , deg	42.735	42.790	42.890	30.525	30.485	35.515
Limits <i>h</i> , <i>k</i> , <i>l</i>	-8 ≤ <i>h</i> ≤ 8, -2 ≤ <i>k</i> ≤ 8, -4 ≤ <i>l</i> ≤ 19	-8 ≤ <i>h</i> ≤ 8, -8 ≤ <i>k</i> ≤ 8, -10 ≤ <i>l</i> ≤ 19	-8 ≤ <i>h</i> ≤ 0, -8 ≤ <i>k</i> ≤ 3, -19 ≤ <i>l</i> ≤ 0	-7 ≤ <i>h</i> ≤ 7, -7 ≤ <i>k</i> ≤ 7, -17 ≤ <i>l</i> ≤ 17	-7 ≤ <i>h</i> ≤ 7, -7 ≤ <i>k</i> ≤ 5, -17 ≤ <i>l</i> ≤ 17	-8 ≤ <i>h</i> ≤ 8, -8 ≤ <i>k</i> ≤ 3, -19 ≤ <i>l</i> ≤ 19
Number of reflections: measured/ unique with <i>I</i> > 2 $\sigma$ ( <i>I</i> )	586/409	541/408	644/408	1991/273	1444/274	1974/414
Number of parameters in refinement	18			16	17	19
Weighting scheme	$1/[\sigma^2(F_0^2) + (0.1048P)^2 + 0.01P]$ , $P = (F_0^2 + 2F_c^2)/3$	$1/[\sigma^2(F_0^2) + (0.1165P)^2 + 0.02P]$ , $P = (F_0^2 + 2F_c^2)/3$	$1/[\sigma^2(F_0^2) + (0.0852P)^2 + 0.02P]$ , $P = (F_0^2 + 2F_c^2)/3$	$1/[\sigma^2(F_0^2) + (0.1482P)^2]$ , $P = (F_0^2 + 2F_c^2)/3$	$1/[\sigma^2(F_0^2) + (0.1451P)^2]$ , $P = (F_0^2 + 2F_c^2)/3$	$1/[\sigma^2(F_0^2) + (0.1482P)^2]$ , $P = (F_0^2 + 2F_c^2)/3$
<i>R</i> <sub>1</sub> ( <i>I</i> > 2 $\sigma$ ( <i>I</i> ))	0.0632	0.0604	0.0604	0.0918	0.0900	0.0962
<i>wR</i> <sub>2</sub>	0.1712	0.1968	0.1698	0.2118	0.2334	0.2335
<i>S</i>	1.260	1.275	1.319	0.993	1.093	1.068
Program	SHELXL-97 [17]					

**Table 4**  
Atomic coordinates, the equivalent isotropic thermal parameters  $U_{eq} \times 10^2$  (Å<sup>2</sup>), the site occupancies p (SOF) and main interatomic distances  $d$  (Å) in the structures of PMWO crystals according to the NDA and XDA data.

Technique	NDA			XDA		
	Sample	PMWO-2	PMWO-3	PMWO-1	PMWO-2	PMWO-3
(Pb, Y) (4a)						
x	01-Feb	01-Feb	01-Feb	01-Feb	01-Feb	01-Feb
y	03-Apr	03-Apr	03-Apr	03-Apr	03-Apr	03-Apr
z	01-Aug	01-Aug	01-Aug	01-Aug	01-Aug	01-Aug
Pb p	0.243(1)	0.240(1)	0.2375(15)	0.245(1)	0.244(2)	0.233(2)
Y p	0.007(1)	0.010(1)	0.0125(15)	0.005(1)	0.006(2)	0.017(2)
$U_{eq}$	1.96(3)	2.00(4)	1.97(4)	0.19(6)	1.02(7)	1.03(2)
(Mo,W,Nb) (4b)						
x	0	0	0	0	0	0
y	01-Apr	01-Apr	01-Apr	01-Apr	01-Apr	01-Apr
z	01-Aug	01-Aug	01-Aug	01-Aug	01-Aug	01-Aug
Mo p	0.122(2)	0.130(2)	0.180(2)	0.075(1)	0.134(1)	0.193(2)
W p	0.121(2)	0.110(2)	0.045(2)	0.175(1)	0.116(1)	0.057(2)
Nb p	0.007(2)	0.010(2)	0.025(2)	— <sup>a</sup>	— <sup>a</sup>	— <sup>a</sup>
$U_{eq}$	1.88(4)	1.86(6)	1.93(4)	0.07(9)	0.9(5)	1.02(7)
O (16f)						
x	0.2344(1)	−0.2345(2)	0.2348(2)	0.234(1)	0.233(2)	0.235(2)
y	0.3891(2)	0.3884(2)	0.3876(2)	0.110(1)	0.390(2)	0.114(2)
z	0.04358(7)	0.04366(9)	0.04390(9)	0.0441(6)	0.0440(8)	0.0444(7)
p	1.00(1)	1.00(1)	0.995(2)	0.9975(20)	0.996(2)	0.990(5)
$U_{eq}$	2.32(3)	2.36(4)	2.30(4)	0.57(14)	1.2(2)	1.0(2)
(Pb, Y)–O × 4	2.6085(9)	2.607(1)	2.604(1)	2.610(7)	2.618(9)	2.611(9)
–O × 4	2.6311(9)	2.631(1)	2.627(1)	2.624(7)	2.623(9)	2.641(9)
[(Pb, Y)–O] <sub>avr</sub>	2.6198	2.619	2.615	2.617	2.6205	2.626
(Mo, W, Nb)–O × 4	1.7804(9)	1.777(1)	1.772(1)	1.773(7)	1.776(9)	1.772(9)

<sup>a</sup> The composition was refined without taking niobium into account.

**Table 5**  
Refined compositions of PMWO crystals determined by the NDA, XDA and RM.

Sample	Refined composition		
	NDA	XDA	RM
PMWO-1	(Pb <sup>2+</sup> <sub>0.972</sub> Y <sup>3+</sup> <sub>0.028(4)</sub> )(Mo <sup>6+</sup> <sub>0.490</sub> W <sub>0.482(8)</sub> Nb <sup>5+</sup> <sub>0.028</sub> )O <sub>4</sub>	(Pb <sup>2+</sup> <sub>0.980(5)</sub> Y <sup>3+</sup> <sub>0.020</sub> )(Mo <sup>6+</sup> <sub>0.300(5)</sub> W <sup>6+</sup> <sub>0.700</sub> )(O <sub>3.990(8)</sub> □ <sub>0.010</sub> ) <sup>a</sup> (Pb <sup>2+</sup> <sub>0.980</sub> Y <sub>0.020</sub> ) [(Mo <sup>6+</sup> , W <sup>6+</sup> ) <sub>0.960</sub> Nb <sup>5+</sup> <sub>0.040</sub> ](O <sub>3.990(8)</sub> □ <sub>0.010</sub> ) <sup>b</sup>	(Pb <sup>2+</sup> <sub>0.988(3)</sub> Y <sup>3+</sup> <sub>0.012</sub> )(Mo <sup>6+</sup> <sub>0.357</sub> W <sub>0.643(9)</sub> )O <sub>4</sub> <sup>a</sup> R <sub>p</sub> = 9.53 R <sub>w-p</sub> = 13.06
PMWO-2	(Pb <sup>2+</sup> <sub>0.960</sub> Y <sup>3+</sup> <sub>0.040(4)</sub> )(Mo <sup>6+</sup> <sub>0.519</sub> W <sub>0.441(8)</sub> Nb <sup>5+</sup> <sub>0.040</sub> )O <sub>4</sub>	(Pb <sup>2+</sup> <sub>0.975(8)</sub> Y <sup>3+</sup> <sub>0.025</sub> )(Mo <sup>6+</sup> <sub>0.536(5)</sub> W <sup>6+</sup> <sub>0.464</sub> )(O <sub>3.985(10)</sub> □ <sub>0.015</sub> ) <sup>a</sup> (Pb <sup>2+</sup> <sub>0.975</sub> Y <sub>0.025</sub> ) [(Mo <sup>6+</sup> , W <sup>6+</sup> ) <sub>0.945</sub> Nb <sup>5+</sup> <sub>0.055</sub> ](O <sub>3.985(10)</sub> □ <sub>0.015</sub> ) <sup>b</sup>	(Pb <sup>2+</sup> <sub>0.979(3)</sub> Y <sup>3+</sup> <sub>0.021</sub> )(Mo <sup>6+</sup> <sub>0.560</sub> W <sub>0.440(8)</sub> )O <sub>4</sub> <sup>a</sup> R <sub>p</sub> = 9.31 R <sub>w-p</sub> = 12.82
PMWO-3	(Pb <sup>2+</sup> <sub>0.950</sub> Y <sup>3+</sup> <sub>0.050(8)</sub> )(Mo <sup>6+</sup> <sub>0.719</sub> W <sub>0.183(8)</sub> Nb <sup>5+</sup> <sub>0.100</sub> )O <sub>4</sub> (O <sub>3.980(10)</sub> □ <sub>0.020</sub> )	(Pb <sup>2+</sup> <sub>0.930(10)</sub> Y <sup>3+</sup> <sub>0.070</sub> )(Mo <sup>6+</sup> <sub>0.770(8)</sub> W <sub>0.230</sub> )(O <sub>3.960(20)</sub> □ <sub>0.040</sub> ) (Pb <sup>2+</sup> <sub>0.930(10)</sub> Y <sup>3+</sup> <sub>0.070</sub> ) [(Mo <sup>6+</sup> , W <sup>6+</sup> ) <sub>0.850</sub> Nb <sub>0.150</sub> ] (O <sub>3.960(20)</sub> □ <sub>0.060</sub> ) <sup>a</sup>	(Pb <sup>2+</sup> <sub>0.962(3)</sub> Y <sup>3+</sup> <sub>0.038</sub> )(Mo <sup>6+</sup> <sub>0.813</sub> W <sub>0.187(8)</sub> )O <sub>4</sub> <sup>a</sup> R <sub>p</sub> = 8.98 R <sub>w-p</sub> = 12.49

<sup>a</sup> The composition was refined without taking niobium into account.

<sup>b</sup> The composition was obtained based on the electroneutrality condition.

(Fig. 2), it is possible that the macropart of PMWO-3 crystal ( $x = 0.8$ ) contains the highest Y and, probably, O vacancies contents. Indeed, as a result of refinement of site occupancies based on the NDA data (Tables 3–5), a partial substitution of Pb<sup>2+</sup> ions by Y<sup>3+</sup> ones was found for all solid solutions; such substitution was greater for PMWO-3 crystal. It should be added that oxygen vacancies were revealed in the composition of its PMWO-3 macropart only (Table 5): (Pb<sup>2+</sup><sub>0.950</sub>Y<sup>3+</sup><sub>0.050(8)</sub>)(Mo<sup>6+</sup><sub>0.719</sub>W<sub>0.183(8)</sub>Nb<sup>5+</sup><sub>0.100</sub>)(O<sub>3.980(10)</sub>□<sub>0.020</sub>). The nuclear scattering factors of Mo ( $b = 0.695$ ) and Nb ( $b = 0.705$ ) are slightly different, that allows to evaluate the Mo, W and Nb contents in tetrahedral sites of macroparts of all solid solutions using the SHELXL97 software package [17]. Correctness of the refined compositions was confirmed by the electroneutrality of systems and correlation between dodecahedral and tetrahedral sites and their interatomic distances (Tables 4, 5). The average

interatomic distances (Pb, Y) – O decrease with decreasing “average radii” of cations in the dodecahedron from PMWO-1 to PMWO-3, which were estimated based on the refined compositions (1.282 Å, 1.279 Å, 1.2765 Å for PMWO-1, PMWO-2, PMWO-3, respectively) (Table 4). The (Mo, W, Nb) – O interatomic distances also decrease with decreasing “average radii” of cations in tetrahedral sites (Table 4). According to the results of the NDA, the defect formation in PMWO-1 and PMWO-2 solid solutions can be written by quasi-chemical equation  $0 \rightarrow Y_{Pb'} + Nb_{(W, Mo)}^{\bullet}$  (Eq. 9), and that in PMWO-3—by  $0 \rightarrow mY_{Pb'} + pNb_{(W, Mo)}^{\bullet} + V_O^{n\bullet}$  ( $m = p + n$ ) (Eq. 10).

Behavior of the unit cell parameters of microparts of PbMo<sub>x</sub>W<sub>1-x</sub>O<sub>4</sub> crystals (XDA) is different from that found by the NDA and RM: a negative deviation of the  $a$  unit cell parameter from the line (Eq. 3) was found for compositions with  $x = 0.2$  and  $0.5$ , and

a positive deviation from this line was found for  $x=0.8$ ; a positive deviation of the  $c$  unit cell parameter from the line (Eq. 4) was found for  $x=0.5$  and a negative deviation from this line was found for  $x=0.2$  and  $0.8$  (Fig. 2a,b). Different types of dependencies of the unit cell parameters of the samples under investigation, which were determined based on different experiments on different objects of the same crystals, show inhomogeneity in composition in  $\text{PbMo}_x\text{W}_{1-x}\text{O}_4$  single crystals.

According to the XDA data (Tables 3–5), the refined composition of the PMWO-3 solid solution with  $x=0.8$  can be written as  $(\text{Pb}^{2+}_{0.930(10)}\text{Y}^{3+}_{0.070})(\text{Mo}^{6+}_{0.770(8)}\text{W}_{0.230})(\text{O}_{3.960(20)})\square_{0.040}$ . The form factor of atoms in the X-ray diffraction experiment is proportional to element number in the periodic Table ( $N_{\text{Pb}}=82, N_{\text{Y}}=39; N_{\text{W}}=74, N_{\text{Mo}}=42, N_{\text{Nb}}=41$ ), and, therefore, it is not possible to refine the  $\text{Nb}^{5+}$  content by the XDA (as well as by the RM). The composition of micropart of the PMWO-3 solid solution is  $(\text{Pb}^{2+}_{0.930(10)}\text{Y}^{3+}_{0.070})[(\text{Mo}^{6+}, \text{W}^{6+})_{0.850}\text{Nb}_{0.150}](\text{O}_{3.960(20)})\square_{0.060}$ , taking into account the electroneutrality of system, i.e. the Nb content in micropart of this crystal is actually higher than that in microparts of other crystals and macropart of the PMWO-3 crystal (Table 5). Thus, quasi-chemical Eq. (10) describes the defect formation of microparts (XDA) of all compositions of solid solutions, which confirms the inhomogeneity in bulk crystals.

The compositions of PMWO solid solutions, refined by the RM, do not contradict the compositions, refined by the NDA and XDA (Table 5), and the behavior of the unit cell parameters of all solid solutions, determined by the NDA, XDA and RM (Tables 2, 5; Fig. 2), confirms the correlation between the unit cell parameters and compositions of the crystallographic sites, determined by the corresponding methods.

According to Table 2, PMO and PWO crystals, grown both in air and in nitrogen atmospheres without adding of  $\text{YNbO}_4$  into initial charge, have light yellow coloration, whereas PMWO crystals, grown from charge with over-stoichiometric amount of  $\text{YNbO}_4$  (15 wt%), are colorless. Based on the results obtained, it can be concluded that the introduction of a buffer component  $\text{Y}^{3+}\text{Nb}^{5+}\text{O}_4$  into the charge  $\text{Pb}^{2+}\text{Mo}^{6+}_x\text{W}^{6+}_{1-x}\text{O}_4$  with  $x=0.2, 0.5$  and  $0.8$  contributes to the compensation of formal charges and growth of colorless crystals (i.e. without color centers). In this case, the assumption of Oeder et al. [23] that the crucible material (Pt) is responsible for yellow coloration of PTO crystals, grown by the Czochralski method, is not confirmed. Furthermore, Kaurova et al. [12] showed that the ordering of oxygen vacancies in the PWO structure results in symmetry reduction from space group  $I4_1/a$  to  $I4$  in a local region of crystals (according to the XDA), caused by kinetic (growth) order-disorder phase transition. In our case, despite the presence of oxygen vacancies in the structures of all microparts of PMWO solid solutions, any change in symmetry was not observed. This fact can be explained by disordering of cations in tetrahedral sites occupied statistically by three types of atoms, Mo, W and Nb.

Introduction of a buffer component  $\text{Y}^{3+}\text{Nb}^{5+}\text{O}_4$  into the  $\text{PbMo}_x\text{W}_{1-x}\text{O}_4$  solid solutions results in difference between the initial charge compositions and refined crystal compositions (the ratio of Mo and W): the Mo contents in refined compositions are higher and less for  $x=0.2$  and  $x=0.8$ , respectively, than those in initial charge; the Mo contents in initial and refined compositions are comparable for  $x=0.5$  (Table 5). Heterovalent substitutions  $\text{Y}^{3+} \rightarrow \text{Pb}^{2+}$  and  $\text{Nb}^{5+} \rightarrow \text{Mo}^{6+}$  result in a self-compensation of electrical neutrality of the system and, probably, to the “balancing” of the sizes of polyhedra: the  $\text{Nb}^{5+}$  and  $\text{Y}^{3+}$  contents ( $r_{\text{Pb}^{2+}} > r_{\text{Y}^{3+}}$ ,  $r_{\text{Nb}^{5+}} > r_{\text{W}^{6+}} > r_{\text{Mo}^{6+}}$ ) as well as oxygen vacancies content increase with increasing  $\text{Mo}^{6+}$  content in  $\text{PbMo}_x\text{W}_{1-x}\text{O}_4$  crystals.

## 4. Conclusions

X-ray and neutron single-crystal and X-ray powder (Rietveld method) diffraction investigations of  $\text{PbMo}_x\text{W}_{1-x}\text{O}_4$  solid solutions with  $x=0.2, 0.5, 0.8$ , grown by the Czochralski method in air atmosphere from the initial charge with over-stoichiometric amount of  $\text{YNbO}_4$  (15 wt%), showed that  $\text{PbMo}_x\text{W}_{1-x}\text{O}_4$  crystals with  $x=0.2, 0.5, 0.8, 1.0$  crystallize in the scheelite-type structure with space group  $I4_1/a$ , unlike the crystal with  $x=0$ , which is characterized by the symmetry reduction to space group  $I4$  caused by ordering of oxygen vacancies.

The correlation between the  $a$  and  $c$  unit cell parameters and compositions of cation sites, dodecahedral and tetrahedral, and the deficiency of the oxygen site was revealed.

Introduction of a buffer component  $\text{YNbO}_4$  into the  $\text{PbMo}_x\text{W}_{1-x}\text{O}_4$  solid solutions contributes to growth of colorless crystals, i.e. without color centers.

It was revealed that the  $\text{Nb}^{5+}$  and  $\text{Y}^{3+}$  contents as well as oxygen vacancies content increase with increasing  $\text{Mo}^{6+}$  content in  $\text{PbMo}_x\text{W}_{1-x}\text{O}_4$  crystals.

## Acknowledgement

We thank the Ministry of Education and Science of Russian Federation for support of this work (No. 4.745.2014/K; 2014–2016). X-ray studies were fulfilled using a STOE STADI VARI PILATUS-100K diffractometer purchased by MSU Development Program.

## References

- [1] A.W. Sleight, Accurate cell dimensions for  $\text{ABO}_4$  molybdates and tungstates, *Acta Cryst. B* 28 (1972) 2899–2902.
- [2] G.A. Coquin, D.A. Pinnow, A.W. Warner, Physical properties of lead molybdate relevant to acousto-optic device applications, *J. Appl. Phys.* 42 (6) (1971) 2162–2168.
- [3] A. Borisevich, A. Fedorov, A. Hofstaetter, M. Korzhik, B.K. Meyer, O. Missevitch, R. Novotny, Lead tungstate scintillation crystal with increased light yield for the PANDA electromagnetic calorimeter, *Nucl. Instr. Methods A* 537 (2005) 101–104.
- [4] F.A. Danevich, B.V. Grinyov, S. Henry, M.B. Kosmyrna, H. Kraus, et al., Feasibility study of  $\text{PbWO}_4$  and  $\text{PbMoO}_4$  crystal scintillators for cryogenic rare events experiments, *Nucl. Instr. Methods A* 622 (2010) 608–613.
- [5] T.T. Basiev, Spectroscopy of new SRS-active crystals and solid-state SRS lasers, *Phys. Usp.* 42 (1999) 1051–1056.
- [6] T.T. Basiev, S.V. Vassiliev, M.E. Doroshenko, et al., Laser and self-Raman-laser oscillations of  $\text{PbMoO}_4:\text{Nd}^{3+}$  crystal under laser diode pumping, *Opt. Lett.* 31 (2006) 65–67.
- [7] T.T. Basiev, M.E. Doroshenko, L.I. Ivleva, V.V. Osiko, M.B. Kosmyrna, et al., Lasing properties of selectively pumped Raman-active  $\text{Nd}^{3+}$ -doped molybdate and tungstate crystals, *Quantum Electron.* 36 (8) (2006) 720–726.
- [8] T.T. Basiev, M.E. Doroshenko, S.N. Smetanin, et al., Multi-wave SRS oscillation in  $\text{PbMoO}_4$  and  $\text{PbMo}_{0.5}\text{W}_{0.5}\text{O}_4$  crystals under 18 picosecond laser pumping, *Laser Phys. Lett.* 9 (2012) 853–857.
- [9] T.M. Bochkova, M.D. Volnyanskii, D.M. Volnyanskii, V.S. Shchetinkin, Color centers in lead molybdate crystals, *Phys. Solid State* 45 (2) (2003) 244–247.
- [10] G.M. Kuz'micheva, V.B. Rybakov, K.A. Subbotin, et al., Colors of mixed-substituted double molybdate single crystals having scheelite structure, *Russ. J. Inorg. Chem.* 57 (2012) 1128–1133.
- [11] Yu.N. Gorobets, I.A. Kaurova, G.M. Kuz'micheva, A.N. Shekhovtsov, V.B. Rybakov, A. Cousson, Influence of the dopant type on point defects in  $\text{PbMoO}_4$  crystals, *J. Surf. Invest. X-ray Synchrotron Neutron Tech.* 8 (4) (2014) 734–744.
- [12] I.A. Kaurova, G.M. Kuz'micheva, A.A. Brykovskiy, V.B. Rybakov, Yu.N. Gorobets, A.N. Shekhovtsov, A. Cousson, Influence of growth conditions on structural parameters of scheelite  $\text{PbTO}_4$  ( $T=\text{Mo}, \text{W}$ ) crystals, *Mater. Des.* 97 (2016) 56–63.
- [13] P. Lecoq, A. Annenkov, A. Gektin, M. Korzhik, C. Pedrini, *Inorganic Scintillators For Detector Systems*, Springer-Verlag Berlin Heidelberg, Berlin, Heidelberg, 2006, doi:http://dx.doi.org/10.1007/3-540-27768-4.
- [14] J. Rodrigues-Carvajal, The programs for rietveld refinement, *Phys. B* 192 (1993) 55–69.
- [15] R.A. Young, A. Sakthivel, T.S. Moss, C.O. Paiva-Santos, Rietveld analysis of X-Ray and neutron powder diffraction patterns. User's guide to program DBWS-9411 (accessed 30.03.95).
- [16] L.J. Farrugia, WinGX suite for small-molecule single-crystal crystallography, *J. Appl. Crystallogr.* 32 (1999) 837–838.
- [17] G.M. Sheldrick, A short history of SHELX, *Acta Crystallogr. A* 64 (2008) 112–122.

- [18] T.I. Mel'nikova, G.M. Kuz'micheva, N.B. Bolotina, V.B. Rybakov, Ya V. Zubavichus, et al., Structural features of compounds of the sillenite family, *Crystallogr. Rep.* 59 (3) (2014) 353–361.
- [19] T.I. Mel'nikova, G.M. Kuz'micheva, N.B. Bolotina, N.V. Sadovskaya, Development of methods of X-ray diffraction analysis for determining the composition and structure of sillenite-family crystals, *Crystallogr. Rep.* 59 (2) (2014) 155–159.
- [20] R.D. Shannon, Revised effective ionic radii and systematic studies of interatomic distances in halides and chalcogenides, *Acta Crystallogr.* A32 (6) (1976) 751–767.
- [21] G.M. Kuz'micheva, S.N. Kozlikin, E.V. Zharikov, S.P. Kalitin, V.V. Osiko, Point defects in gadolinium gallium garnet, *Zhurnal Neorganicheskoi Khimii (Russ. J. Inorg. Chem.)* 33 (9) (1988) 33–39.
- [22] E.A. Tyunina, I.A. Kaurova, G.M. Kuz'micheva, V.B. Rybakov, A. Cousson, O. Zaharko, Diffraction methods for determination of composition and structural parameters of langasite family compounds, *Vestnik MITHT (Fine Chemical Technol.)* 5 (1) (2010) 57–68.
- [23] R. Oeder, A. Scharmann, D. Schwabe, B. Vitt, Growth and properties of  $\text{PbWO}_4$  and  $\text{Pb}(\text{WO}_4)$ - $(\text{MoO}_4)$  mixed crystals, *J. Cryst. Growth* 43 (1978) 537–540.